

Rod-shaped Fe₂O₃ Efficiently Catalyzes Selective Reduction of Nitrogen Oxide by Ammonia**

Xiaoling Mou, Bingsen Zhang, Yong Li, Lide Yao, Xuejiao Wei, Dang Sheng Su*, and Wenjie Shen*

Selective catalytic reduction (SCR) of nitrogen oxides (NO_x) with NH₃ is nowadays the most promising technology for eliminating nitrogen oxides that are emitted from combustion of fossil fuels.^[1] Vanadia-based catalysts are commonly used for this reaction in stationary sources, like coal-fired power plant and energy use in industry. This mature system displays adequate activity typically at 300–400 °C, but is still not satisfactory with respect to the volatility and toxicity of VO_x and the easy deactivation.^[1–3] Attracted by the inherently environmental-benign character and the prominent thermal stability, ferric oxides have long been explored to catalyze selective reduction of NO_x with ammonia,^[3,4–8] but no significant progress has been achieved by far. They are commonly featured by insufficient activity at low temperatures and severe deactivation induced by H₂O and SO₂ that are permanently and abundantly present in the exhaust. On the other hand, studies on crystal phase and shape control of Fe₂O₃ nanomaterials are of great interest in materials science and are actively being pursued in recent years.^[9–14] However, most of the synthetic strategies involve high-temperature treatments, yielding undesired mixtures of ferric oxide polymorphs due to diverse phase transitions.^[9] To date, there still remains a challenge to effectively tailor the shape and the crystal phase of Fe₂O₃ materials at nanometer level. Here, we show that γ -Fe₂O₃ nanorods, which preferentially expose the reactive facets by crystal phase and morphology control through a solution-based approach, efficiently catalyze selective reduction of NO with NH₃.

We started with shape-controlled synthesis of β -FeOOH nanorods by precipitation of ferric chloride with sodium carbonate in aqueous solution containing poly ethylene glycol (PEG) at 120 °C. Scanning electron microscopy (SEM) and transmission electron microscopy (TEM) micrographs identify that the obtained β -FeOOH has a rod-like structure with a diameter of 30–50 nm and a length of 350–500 nm (Figure. S1 in the supporting information). When viewed along

the [10̄,1] (Figure 1a) and [100] (Figure 1b) directions by means of high-resolution TEM (HRTEM), the nanorod dominantly exposes the {010} planes. Together with the square-shaped cross section (Figure S1), the β -FeOOH nanorod is determined to be a rectangular block that is enclosed by two {100} flat planes, two {010} side planes, and two {001} end planes (Figure 1c).

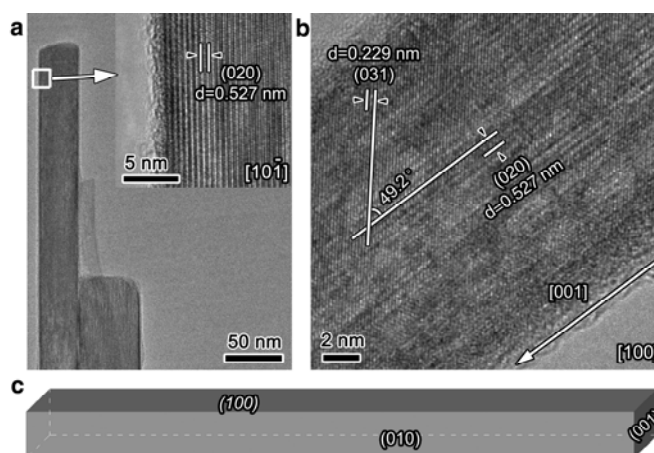


Figure 1. a) A low-magnification TEM image of a single β -FeOOH nanorod viewed along the [10̄,1] direction, the insert HRTEM image indicates that the nanorod exposes the {010} planes. b) Another HRTEM image viewed along the [100] orientation, also showing the preferential exposure of the {010} planes. c) The real shape of the β -FeOOH nanorod.

Gamma-Fe₂O₃ nanorods were then obtained by refluxing the β -FeOOH precursor in PEG at 200 °C. X-ray powder diffraction (XRD) pattern (Figure S2) identifies that the diffraction lines of the (400) and (440) planes are intensified significantly whereas those of the (422) and (511) planes are weakened considerably, as compared to the standard powder reflection pattern, indicative of anisotropic growth of the {110} and {100} planes. SEM and TEM observations reveal that the γ -Fe₂O₃ nanorods have an average diameter of 40 nm and a mean length of 400 nm (Figure S3). Moreover, the γ -Fe₂O₃ nanorods have mesopores of about 22 nm in diameter that have open structures and are isolated from each other, yielding a high surface area of 120 m²/g. Iron oxyhydroxide can be easily dehydrated into iron oxide, but the crystal phase varies largely, depending on the rearrangement of Fe³⁺ and O²⁻ ions.^[15] β -FeOOH has the least dense crystalline structure among its polymorphs and usually dehydrates to α -Fe₂O₃ upon heating.^[16] We obtain, as expected, α -Fe₂O₃ nanorods by calcining the β -FeOOH precursor at 500 °C in air (Figure S4). When refluxed in PEG, surprisingly, the β -FeOOH precursor is converted to γ -Fe₂O₃ nanorods owing to the moderate water removal manner that benefits the crystallization of maghemite. Ferric oxide has four polymorphs and the phase transition is strongly dependent on the size of the particles, especially at nanometer level.^[9,17,18] Hence, we examined the phase stability of the γ -Fe₂O₃ nanorods by *in situ* XRD experiment (Figure S5). The characteristic (311) and (400) diffraction lines of γ -Fe₂O₃ keep stable up to 600 °C with only

[*] X. Mou, Dr. Y. Li, X. Wei, Dr. W. Shen
State Key Laboratory of Catalysis, Dalian Institute of Chemical Physics, Chinese Academy of Sciences, Dalian 116023, China
E-mail: shen98@dicp.ac.cn

Dr. B. Zhang, Dr. D. S. Su
Shenyang National Laboratory for Materials Science, Institute of Metal Research, Chinese Academy of Sciences, Shenyang 110016, China

Dr. L. Yao, Dr. D. S. Su
Department of Inorganic Chemistry, Fritz-Haber Institute of the Max Planck Society, Faradayweg 4-6, 14195 Berlin, Germany
E-mail: dangsheng@fhi-berlin.mpg.de

[**] We acknowledge the financial support for this research work from the National Nature Science Foundation of China (20923001, 21025312).

Supporting information for this article is available on the WWW under <http://www.angewandte.org> or from the author.

slightly weakened intensities. Moreover, the rod-shape is also well maintained even if the γ -Fe₂O₃ nanorods were calcined at 550 °C for 5 h in air. All these results evidence the exceptionally high crystal

phase and shape stabilities of the γ -Fe₂O₃ nanorods raised by the unique morphological feature.

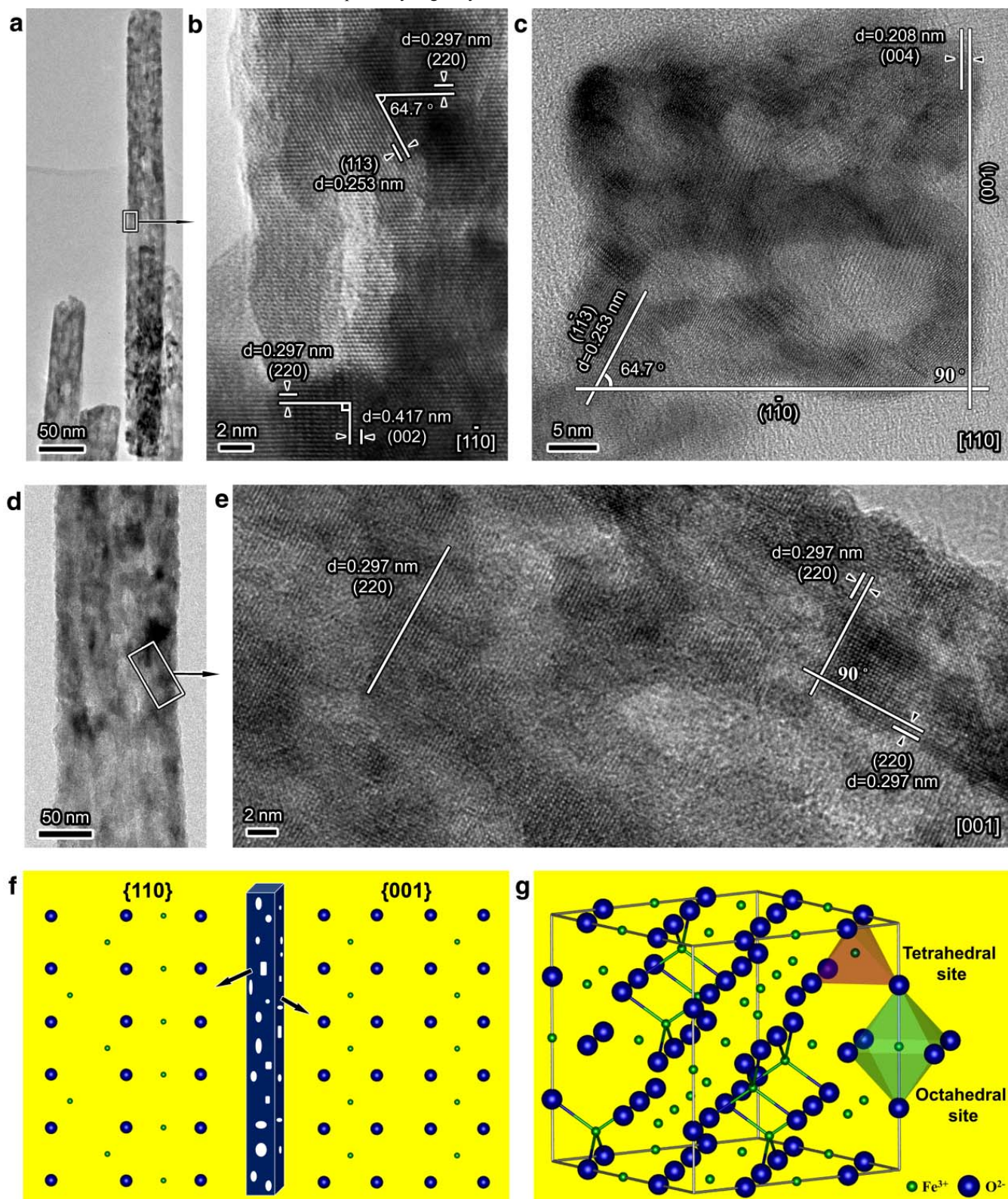


Figure 2. a) Low- and b) high-magnification TEM images of a single γ -Fe₂O₃ nanorod, indicating the dominant exposure of the {110} and {001} planes. c) A square-shaped cross-section of the single rod near the [110] orientation, which is constructed by two side ($\bar{1}$, 10) and (001) planes with a lattice angle of 90°. d) Low- and e) high-magnification TEM images of another γ -Fe₂O₃ nanorod viewed along the [001] direction where the (220) planes are preferentially exposed. f) The real shape of the nanorod and the surface atomic configurations of the preferentially exposed {110} and {001} planes. g) Atomic illustration of a cubic symmetry (space group $Fd\bar{3}m$) and the coordination patterns of tetrahedral and octahedral Fe³⁺ ions.

The crystallographic nature of the γ -Fe₂O₃ nanorods was further examined by HRTEM. Figure 2a shows a single γ -Fe₂O₃ nanorod growing along the [1 $\bar{1}$,10] direction. The interplanar distances of 0.253, 0.297, and 0.417 nm on the enlarged image (Figure 2b) correspond to the lattice fringes of the {113}, {110}, and {001} planes, respectively. The square-shaped cross section viewed near the [110] orientation is constructed by (1 $\bar{1}$,10) and (001) as side planes (Figure 2c). When viewed along the [001] direction, the nanorod dominantly exposes the {110} planes (Figure 2d,e). Taking all the analyses into account, the nanorod is constructed with two {110} as end planes, and two {110} and two {001} as side planes (Figure 2f). It is noteworthy that these surfaces are terminated simultaneously by Fe³⁺ and O²⁻ sites.^[19-21] There are equal numbers of octahedral and tetrahedral Fe³⁺ ions on the {110} plane (4.05 atoms per nm²), but only octahedral Fe³⁺ ions on the {001} plane (5.72 atoms per nm²) (Figure 2g and Figure S3). Consequently, the surface of the γ -Fe₂O₃ nanorod is relatively rich in octahedral Fe³⁺ ions, and more importantly, the length of the Fe-O bond (0.2091 nm) is greater than that in the tetrahedrally coordinated environment (0.1837 nm),^[20] making it more reducible and reactive.

Figure 3a shows the catalytic performance of the γ -Fe₂O₃ nanorods in SCR of NO with NH₃. The light-off temperature (the temperature at which the conversion of NO reaches 50%) is as low as 170 °C and 100% NO conversion is achieved at 220 °C. The temperature window for 80% NO conversion ranges from 200 to 400 °C and the selectivity towards N₂ maintains at about 98% in the whole temperature range (Figure S6). This salient performance is of utmost importance in NO_x-removal at low to medium temperatures. When compared to the industrially used VO_x-based catalysts,^[22,23] the less costly and non-toxic Fe₂O₃ nanorods offer fairly compatible or even slightly better efficiency under similar reaction conditions (Figure S7). As the exhaust usually contains a large amount of H₂O (2-15 vol.%) and certain amounts of SO₂ (30-2000 ppm),^[2,24] we further tested the Fe₂O₃ nanorods with a feed stream containing 10 vol.% H₂O and 100 ppm SO₂. Due to the adsorption of water on the catalyst surface, the light-off temperature increases to 260 °C and the temperature region for 80% NO conversion shifts to 300-500 °C (Figure 3a). Nevertheless, the pronounced activity and the available temperature window still fulfill the criteria for practical stationary NO_x-removal.^[2]

In addition, the γ -Fe₂O₃ nanorods are very robust both in transient process with frequent variation in temperature and in long-term steady operation at a constant temperature. Upon periodically fluctuating the reaction temperature in the range of 150-450 °C, the conversion of NO and the selectivity of N₂ are well reproducible; the temperature region for 80% NO conversion remains at 200-400 °C, and the size and shape of the used catalyst keeps unchanged (Figure S8). When used for a long-term test at 350 °C, a typical temperature in practical applications, NO conversion maintains at 100% for 150 hours (Figure 3b). The addition of H₂O and SO₂ slightly lowers NO conversion to about 90%, but the removal of SO₂ from the reaction gas immediately raises NO conversion to 93%. After cutting off the supply of water, the conversion of NO rapidly restores to 100% and keeps at this level for the rest operation. This reaction pattern demonstrates that the γ -Fe₂O₃ nanorods are highly sulfur-resistant and the inhibition of water is reversible, differing from the traditional iron oxides that are severely and irreversibly deactivated by H₂O and SO₂.^[5,6] TEM analyses of the catalyst after the stability test confirm that both the morphology and the exposed facets are almost the same as the fresh one (Figure 3c). Electron energy loss spectroscopy (EELS) reaffirms that the oxidation state of iron and the coordination of oxygen in the catalyst keep

unchanged before and after the reaction (Table S1 in the supporting information), indicating the stable surface coordination environment.

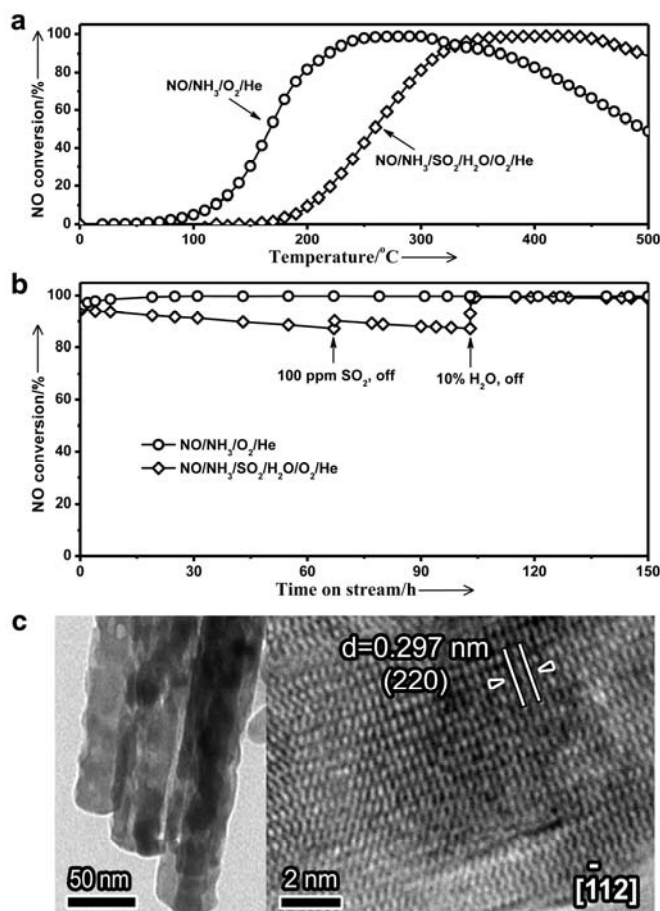


Figure 3. a) NO conversion as a function of temperature with (circle) and without (square) water (10 vol. %) and SO₂ (100 ppm) in the feed gas of 1000 ppm NO/1000 ppm NH₃/3.0 vol.% O₂/He (72000 ml.g⁻¹.h⁻¹). b) Stability tests at 350 °C for 150 hours. c) TEM images of the used catalyst.

Activation of NH₃ on the catalyst surface is generally viewed as the primary step in SCR of NO, as being experimentally identified on VO_x-based catalysts.^[25-27] Temperature-programmed desorption (TPD) of NH₃ on the γ -Fe₂O₃ nanorods shows an intense desorption peak of N₂ at 250-430 °C (Figure 4a). Since there is no oxygen in the feed gas, the generation of nitrogen is originated from the oxidation of adsorbed ammonia by the lattice oxygen of γ -Fe₂O₃. This is also supported by the TPD profile of NH₃/O₂ co-adsorption where the pre-adsorbed molecular oxygen has negligible impact on the desorption pattern of N₂ (Figure 4b). In fact, the Fe₂O₃ nanorods catalyze NH₃ oxidation very efficiently; the conversion of NH₃ and the selectivity towards N₂ are as high as 90% even at 350 °C (Figure S9), evidencing the facile activation of ammonia. On the other hand, the adsorption of NO is strongly affected by the presence of oxygen molecule. NO is only weakly adsorbed on the Fe₂O₃ nanorods and is easily desorbed below 250 °C (Figure 4c). However, the presence of molecular oxygen greatly promotes the adsorption of NO. The co-adsorption of NO/O₂ yields a strong desorption peak of NO₂ at 372 °C (Figure 4d). This is in accord with a comparative test of NO oxidation on the Fe₂O₃ nanorods where the conversion of NO to NO₂ reaches 26% at about 370 °C (Figure S9), suggesting that the γ -Fe₂O₃ nanorods enable to catalyze NO oxidation effectively as well.

Catalytically, the outstanding SCR performance of the γ -Fe₂O₃ nanorods is intimately associated with the exposed {100} and {001} planes. Ammonia is adsorbed on the Lewis acid site in association

with ferric cation while NO is weakly adsorbed on Fe³⁺ site.^[28-30] The inferior performance of the α -Fe₂O₃ nanorods in a comparative test confirms that the exposed {2⁻10} and {001} planes are less active (Figure S4d,e). This is because these Fe-terminated surfaces in the α -phase (space group $R\bar{3}ch(167)$) only provide ferric sites for the adsorptions of NO and NH₃ but lack neighboring oxygen anions for their activations. In contrast, the {110} and {001} surfaces on the γ -Fe₂O₃ nanorods contain iron and oxygen ions simultaneously. The acidic ferric site and its neighboring basic oxygen site jointly accomplishes the reactive adsorptions of NO and NH₃, and their subsequent reaction yields nitrogen and water, probably through surface nitrates.^[27] The apparent activation energies are 49 and 56 kJ/mol at 120-160 °C and 340-360 °C, respectively. The turnover frequencies of the Fe³⁺ site are $1.39 \times 10^{-3} \text{ s}^{-1}$ at 150 °C and $6.01 \times 10^{-3} \text{ s}^{-1}$ at 350 °C (Table S2 in the supporting information).

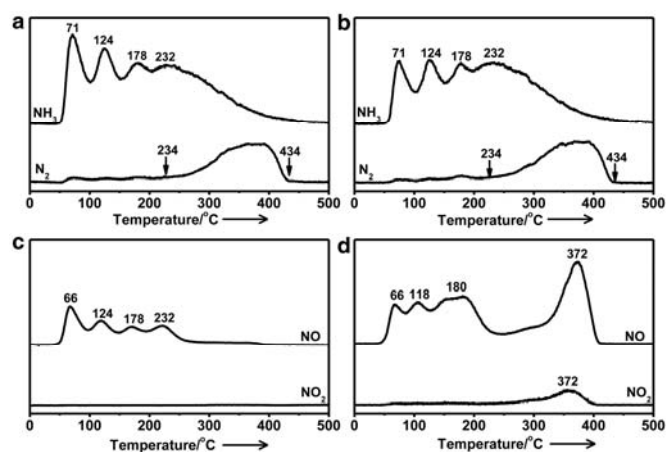


Figure 4. TPD profiles of a) NH₃, b) NH₃/O₂, c) NO, and d) NO/O₂ on the γ -Fe₂O₃ nanorods.

In summary, we have successfully fabricated crystal phase and morphology controlled Fe₂O₃ nanomaterials. In particular, γ -Fe₂O₃ nanorods that are enclosed by the reactive {110} and {100} facets are highly active and distinctively stable for SCR of NO with NH₃. This offers a possibility for obtaining highly efficient SCR catalysts using less costly and non-toxic Fe₂O₃ nanomaterials, and raises a new strategy more generally to promote the catalytic property of metal oxides by tuning crystal phase and shape at nanometer level.

Experimental Section

Materials preparation. The β -FeOOH nanorods were prepared by an aqueous precipitation method. An aqueous solution containing 5.38 g of FeCl₃·6H₂O, 11.60 g of NaCl, 10 ml of poly ethylene glycol (PEG) and 190 ml of water was gradually heated to 120 °C. 200 ml of 0.2 M Na₂CO₃ aqueous solution was then added through a syringe pump at a rate of 5.5 ml/min. The mixture was aged at 120 °C for 1 h. The precipitate was washed with water and ethanol, and finally dried at 50 °C for 6 h in vacuum. The γ -Fe₂O₃ nanorods were prepared by refluxing the β -FeOOH precursor in PEG. A slurry mixture containing 5.0 g of β -FeOOH nanorods and 500 ml of PEG was gradually heated to 200 °C and refluxed for 24 h under nitrogen flow. The resulting solid was washed with water and ethanol, followed by drying at 50 °C for 12 h in vacuum.

Structure analyses. TEM images were taken on a Philips FEI Tecnai G² microscopy operating at 120 kV. HRTEM images were recorded on a FEI Cs-corrected Titan 80-300 microscope operated at 300 kV with a Gatan Filter. EELS analyses were performed with an energy dispersion of 0.1 eV. TPD of NO and NH₃ on the γ -Fe₂O₃ nanorods were conducted with a quartz tubular reactor connected to a mass spectrometer. 100 mg samples were pre-treated with a 3.0

vol.% O₂/He mixture at 400 °C for 0.5 h, followed by NH₃ or NO adsorption at room temperature.

Catalytic evaluation. SCR of NO with NH₃ was conducted with a continuous-flow quartz tubular reactor under atmospheric pressure. Before the test, 100 mg of γ -Fe₂O₃ nanorods (40–60 mesh) were treated with a 3.0 vol.% O₂/He mixture (60 ml/min) at 400 °C for 0.5 h. Typically, the feed gas contained 1000 ppm NO, 1000 ppm NH₃, and 3 vol.% O₂ balanced with He (120 ml/min). When necessary, 10.0 vol.% H₂O and 100 ppm SO₂ were added to the gas stream. The concentrations of nitrogen oxides and nitrogen in the inlet and outlet streams were continuously detected by a NO/NO_x analyzer and a mass spectrometer.

Received: ((will be filled in by the editorial staff))

Published online on ((will be filled in by the editorial staff))

Keywords: crystal phase · ferric oxide · heterogeneous catalysis · morphology control · nanorods · NO_x-removal

- [1] S. Roy, M. S. Hegde, G. Madras, *Appl. Energy* **2009**, *86*, 2283-2297.
- [2] E. Hums, *Catal. Today* **1998**, *42*, 25-35.
- [3] R. M. Heck, *Catal. Today* **1999**, *53*, 519-523.
- [4] G. Busca, L. Lietti, G. Ramis, F. Berti, *Appl. Catal. B-Environ.* **1998**, *18*, 1-36.
- [5] N. Apostolescu, B. Geiger, K. Hizbullah, M. Jan, S. Kureti, D. Reichert, F. Schott, W. Weisweiler, *Appl. Catal. B-Environ.* **2006**, *62*, 104-114.
- [6] Z. Liu, P. J. Millington, J. E. Bailie, R. R. Rajaram, J. A. Anderson, *Microporous Mesoporous Mat.* **2007**, *104*, 159-170.
- [7] F. Liu, H. He, C. Zhang, *Chem. Commun.* **2008**, 2043-2045.
- [8] G. H. Yao, K. T. Gui, F. Wang, *Chem. Eng. Technol.* **2010**, *33*, 1093-1098.
- [9] L. Machala, J. Tuček, R. Zboržil, *Chem. Mater.* **2011**, *23*, 3255-3272.
- [10] Y. Piao, J. Kim, H. B. Na, D. Kim, J. S. Baek, M. K. Ko, J. H. Lee, M. Shokouhimehr, T. Hyeon, *Nat. Mater.* **2008**, *7*, 242-247.
- [11] A. Shavel, L. M. Liz-Marzan, *Phys. Chem. Chem. Phys.* **2009**, *11*, 3762-3766.
- [12] H. G. Cha, S. J. Kim, K. J. Lee, M. H. Jung, Y. S. Kang, *J. Phys. Chem. C* **2011**, *115*, 19129-19135.
- [13] S. Li, H. Zhang, J. Wu, X. Ma, D. Yang, *Cryst. Growth Des.* **2006**, *6*, 351-353.
- [14] F. Meng, S. A. Morin, S. Jin, *J. Am. Chem. Soc.* **2011**, *133*, 8408-8411.
- [15] R. M. Cornell, U. Schwertmann, *the iron oxides: structure, properties, reactions, occurrence and uses*, (2nd edition), *Chapt. 14*, Wiley-VCH, Weinheim, **2003**, pp. 365-405.
- [16] N. K. Chaudhari, J. S. Yu, *J. Phys. Chem. C* **2008**, *112*, 19957-19962.
- [17] S. Sakurai, A. Namai, K. Hashimoto, S. Ohkoshi, *J. Am. Chem. Soc.* **2009**, *131*, 18299-18303.
- [18] A. Navrotsky, L. Mazeina, J. Majzlan, *Science* **2008**, *319*, 1635-1638.
- [19] R. J. Armstrong, A. H. Morrish, G. A. Sawatzky, *Phys. Lett.* **1966**, *23*, 414-416.
- [20] J. E. Jørgensen, L. Mosegaard, L. E. Thomsen, T. R. Jensen, J. C. Hanson, *J. Solid State Chem.* **2007**, *180*, 180-185.
- [21] V. Petkov, P. D. Cozzoli, R. Buonsanti, R. Cingolani, Y. Ren, *J. Am. Chem. Soc.* **2009**, *131*, 14261-14266.
- [22] R. Q. Long, R. T. Yang, *J. Catal.* **1999**, *188*, 332-339.
- [23] H. S. Yang, S. L. Song, H. C. Choi, I. S. Nam, H. J. Chae, *US patent 2002/6475944 B1*.
- [24] K. Skalska, J. S. Miller, S. Ledakowicz, *Sci. Total Environ.* **2010**, *408*, 3976-3989.
- [25] N. Y. Topsoe, *Science* **1994**, *265*, 1217-1219.
- [26] I. Giakoumelou, C. Fountzoula, C. Kordulis, S. Boghosian, *J. Catal.* **2006**, *239*, 1-12.
- [27] A. Grossale, I. Nova, E. Tronconi, D. Chatterjee, M. Weibel, *J. Catal.* **2008**, *256*, 312-322.
- [28] C. H. Rochester, S. A. Topham, *J. Chem. Soc. Faraday Trans.* **1979**, *75*, 1259-1267.
- [29] Y. Wang, Z. Lei, B. Chen, Q. Guo, N. Liu, *Appl. Surf. Sci.* **2010**, *256*, 4042-4047.
- [30] K. Otto, M. Shelef, *J. Catal.* **1970**, *18*, 184-192.

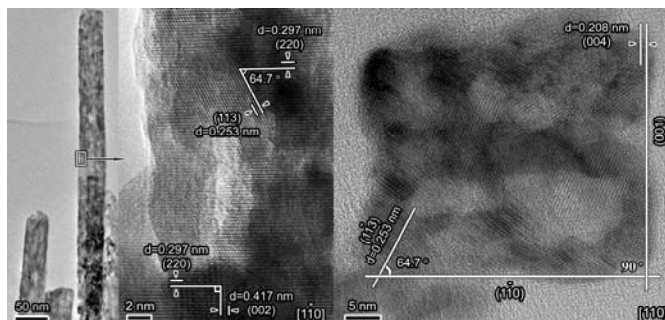
Entry for the Table of Contents

Rod-Shaped Iron Oxide

Xiaoling Mou, Bingsen Zhang, Yong Li,
Lide Yao, Xuejiao Wei, Dang Sheng
Su*, and Wenjie Shen*

Page – Page

Rod-shaped Fe_2O_3 efficiently catalyzes
selective reduction of nitrogen oxide by
ammonia



Rod-shaped Iron Oxide: Fe_2O_3 nanomaterials with controllable crystal phase and morphology have been successfully fabricated, and the $\gamma\text{-Fe}_2\text{O}_3$ nanorods that are enclosed by the reactive $\{110\}$ and $\{100\}$ facets are highly active and distinctively stable for selective catalytic reduction of NO with NH_3 .